photonics

MDPI

Article

Quantum Nonlinear Nonreciprocity in a Cavity-Coupled Quantum Dot–Metal Nanoparticle Hybrid System

Zeyou Li [1], Han Yang [1], Fei Xu [1], Peng Wang [2] and Yihong Qi [1,*]

[1] School of Physics, East China University of Science and Technology, Shanghai 200237, China; zeyou.li22@imperial.ac.uk (Z.L.); y30241323@mail.ecust.edu.cn (H.Y.); xfei@ecust.edu.cn (F.X.)
[2] School of Electronic Engineering and Intelligent Manufacturing, Anqing Normal University, Anqing 246113, China; wangp@aqnu.edu.cn
* Correspondence: qiyihonggl@163.com

Abstract

Optical nonreciprocity (ONR) plays an important role in laser technique, optical communications, quantum information, etc. Realizing ONR at the quantum level of few photons or single photons is also essential for quantum communications or quantum networks. In this work, we propose a hybrid configuration composed of a quantum dot–metallic nanoparticle (QD-MNP) composite in a ring cavity to achieve ONR at the few-photon level via optical bistability. With the surface plasmon effect of the MNP, the bistable property and regime of photons producing ONR in an asymmetric ring cavity including a QD and an MNP inside can be significantly improved in comparison with the case of a single QD. By using the bistability effect, giant ONR can be achieved in an optimal window of numbers of input photons. The detuning and the coupling strength coefficients of the hybrid system can be adjusted and utilized to optimize the performance of the quantum nonreciprocity. This work may find promising applications in quantum nonreciprocal devices and photonic quantum circuits.

Keywords: optical nonreciprocity; single-photon; optical bistability; surface plasmon

1. Introduction

Generally speaking, light transmission follows the Lorentz reciprocity principle in a usual optical medium, i.e., light has the same propagation property in the two reverse directions of the medium [1,2]. Reciprocity is a common phenomenon in the world of light. However, in many photonic systems, suppression of backward signal propagation is highly desirable in order to prevent unwanted reflections, feedback, and noise, especially in optical communication and integrated photonic devices [3]. This requirement has stimulated extensive studies on optical nonreciprocity (ONR) and related nonreciprocal optical devices, such as optical isolators and circulators [4]. These devices allow light transmission in one direction while suppressing propagation in the reverse direction. The magneto-optical effect was first employed to realize the optical nonreciprocity by using the Faraday rotation of polarization [5,6]. Although the magneto-optical nonreciprocal devices are relatively straightforward to implement, the magnetic response of general optical materials is weak, and the large magnetic field and material size also limit its further development in on-chip integration as well as its application in some nonmagnetic environments. Therefore, nonmagnetic approaches for realizing ONR have attracted increasing attention in recent years [7,8].

Check for updates

Received: 13 May 2026
Revised: 4 June 2026
Accepted: 5 June 2026
Published: 9 June 2026

Copyright: © 2026 by the authors. Licensee MDPI, Basel, Switzerland. This article is an open access article distributed under the terms and conditions of the Creative Commons Attribution (CC BY) license.

Some novel mechanisms have been proposed to achieve ONR without the use of a magnetic field, including spatiotemporal modulation of the refractive index [9–11], macroscopic motion of medium [12–14], optical nonlinearity [15–19], optomechanical interaction [20–25], chiral quantum optics [26–28], atomic thermal motion [29–35], etc. Among these techniques, optical nonlinearity, such as Kerr or Kerr-like nonlinearity [36,37], provides an important mechanism for realizing ONR and nonreciprocal optical devices [15–17,38–40]. In particular, nonlinear optical systems based on intrinsic material responses offer a promising route toward passive nonreciprocal photonic devices without relying on magnetic modulation [41,42]. In general, nonlinearity-based ONR requires a large number of photons or high-intensity light to participate in the interaction process. Therefore, generating giant nonlinearity under low light intensity or few photons is an important challenge. Another key issue is to enhance the forward transmittance and isolation contrast at low light levels. Nonlinear optical cavities provide an effective platform for enhancing light–matter interactions, thereby strengthening optical nonlinearity and reducing the photon number required for realizing ONR [43–45].

Surface plasmon in a hybrid system of metallic nanostructures such as metallic nanoparticles (MNPs) and quantum emitters (QEs), including quantum dots (QDs), can effectively enhance nonlinear interaction between light and medium via the local field effect [46–48], which originates from the role of three parts: the direct effect of the applied field, the effect of the polarization field of the MNP and additional feedback effect of QE (the polarization of the QE acts on the MNP and then induces a feedback effect on QE) [49,50]. Thus the plasmon–exciton hybridization of QEs-MNPs causes nanoscale interaction of the light and QEs and provides an ideal solid-state candidate for study of fundamental quantum optical phenomena and fabrication of nanoscale quantum devices [51–53]. Some novel and intriguing quantum optical phenomena have been explored in such hybrid QD-MNP systems, such as plasmon-induced transparency [54,55], vacuum Rabi splitting [56,57], Fano-type absorption spectra [58,59], controllable excitonic population and energy transfer [60–62], and electromagnetically induced grating [63]. Significant enhancement of optical nonlinearity have also been demonstrated by the surface plasmon effect in hybrid QD-MNP systems [64,65].

Because of their potential applications in quantum information and communications, quantum nonreciprocity and nonreciprocal transmission of few photons have attracted great research interest in recent years [35,66–73]. In this work, we investigate optical nonreciprocal transmission at the few-photon level in a single QD-MNP-composed hybridization inside a ring cavity. By calculating the input–output relation of the hybrid cavity, we show that optical nonreciprocity can be realized at the few-photon level in the hybrid system under appropriate parameter conditions. Compared with the single-QD system, the introduction of QD-MNP hybridization not only reduces the required photon numbers for ONR, but also enhances the forward transmittance and isolation performance. This work may be useful for the development of ultracompact nonreciprocal quantum devices.

2. Model and Equations

We consider the coupled ring cavity system as shown in Figure 1a, where a single QD-MNP hybrid is embedded in an asymmetric ring cavity. The cavity mirrors M_1 and M_2 are of partial reflection with different reflectivity, and the cavity mirror M_3 is of total reflection. Loss rates of the cavity mirrors M_1 and M_2 are k_1 and k_2. The forward/backward denotes two reverse propagation directions of the light. Figure 1b shows the detail of the interaction model between light (cavity mode) and the hybrid system. The quantum dot has two states denoted by the ground state $|g\rangle$ and excited state $|e\rangle$, with the transition frequency ω_a between the two states. The red and blue pellets in the cavity represent, respectively, the

quantum dot and the metallic nanoparticle. It is assumed that the coupling strengths among the quantum dot, the MNP and the cavity of frequency ω_c are G, J and Ω, respectively.

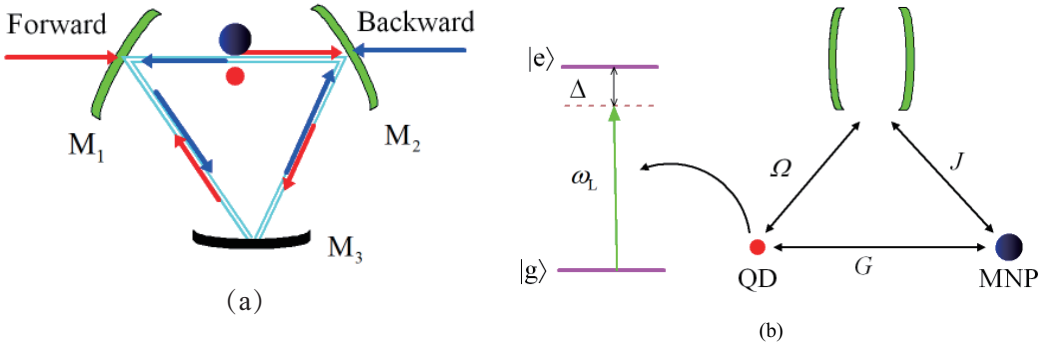


Figure 1. (Color online) proposed configuration and theoretical model. (**a**) Interaction between light and the single QD-MNP hybrid embedded in a ring cavity, (**b**) two-level model of the QD and coupling model of the QD-MNP hybrid and the cavity mode.

For the input photons of frequency ω_L, the interacting Hamiltonian of the system can be described by the following equation in the rotating frame [74,75]:

$$\begin{aligned} H_{\text{acm}} = \quad & \hbar\Delta S_z + \hbar(\Delta+\delta)a^\dagger a + \hbar(\Delta+\delta){d_m}^\dagger d_m + \hbar G(S_+ d_m + {d_m}^\dagger S_-) \\ + \quad & \hbar J({d_m}^\dagger a + a^\dagger d_m) + \hbar\Omega(S_+ a + a^\dagger S_-), \end{aligned} \tag{1}$$

where a and d_m are the annihilation operators of the cavity mode and the MNP. $S_- = |g\rangle\langle e| = S_+^\dagger$ is the lowering operator, and $S_z = (|e\rangle\langle e| - |g\rangle\langle g|)/2$ is the pseudospin operator of the quantum dot. $\Delta = \omega_a - \omega_L$ is the detuning between quantum dot transition and the input field. $\delta = \omega_c - \omega_a$ is the detuning between the cavity mode and the quantum dot transition frequency. J denotes the coupling coefficient between the MNP and the cavity and G (Ω) indicates the coupling coefficient between the quantum dot and the MNP (cavity).

The relationship between the input field b_{in} and the transmitted field b_t can be derived via the cavity input–output calculation [76]. For simplicity, we define the expectation values of these operators as $s = \langle S_-\rangle$, $s_z = \langle S_z\rangle$, $a = \langle a\rangle$, $d_m = \langle d_m\rangle$, $b_{in} = \langle b_{in}\rangle$ and $b_t = \langle b_t\rangle$. For notational simplicity, the same symbols are subsequently used to denote these expectation values. Then, corresponding Heisenberg–Langevin equations can be obtained by substituting the above Hamiltonian into the Heisenberg time evolution equation as follows [77]:

$$\dot{s} = -(i\Delta + \gamma_e/2)s + 2is_z(\Omega a + Gd_m), \tag{2}$$

$$\dot{s}_z = -i\Omega s^+ a + i\Omega s a + iG{d_m}^+ s - iGd_m s^+ - \gamma_e(s_z + 1/2), \tag{3}$$

$$\dot{a} = -i(\Delta+\delta)a - (k + \gamma_{\text{cav}}/2)a - i\Omega s - iJd_m - i\sqrt{k_1}b_{in}, \tag{4}$$

$$\dot{d}_m = i(\Delta+\delta)d_m - iJa - iGs, \tag{5}$$

$$b_t = -i\sqrt{k_2}a, \tag{6}$$

where k_1 and k_2 denote the loss rates of the two asymmetric cavity mirrors M_1 and M_2, respectively, and $k = (k_1 + k_2)/2$ represents the average external cavity decay rate. Here, γ_{cav} is the intrinsic cavity mode loss rate and the $\gamma_e = \gamma_{\text{at}} + \gamma_{\text{am}}$ represents the total decay rate of QD with the QD spontaneous decay rate γ_{at} and loss rate γ_{am} originated from the coupling of QD and MNP. In the calculation, we introduce the average photon number operators $n_{in} = \langle b_{in}^+ b_{in}\rangle$, $n_t = \langle b_t^+ b_t\rangle$ and $n_c = \langle a^+ a\rangle$ for the incident, transmitted and cavity photons respectively. We can obtain the input–output relation of n_{in} and n_t via

solving the Heisenberg–Langevin equations under steady-state condition. It is anticipated that, when the system works in a nonlinear region, ONR can be achieved via the optical bistable process.

From Equation (2), the steady-state dipole moment s of QD and its complex conjugate operator s^+ can be solved as

$$s = \frac{2is_z(\Omega a + Gd_m)}{(i\Delta + \gamma_e/2)} = \frac{(\Omega a + Gd_m)(2\Delta + i\gamma_e)}{\Delta^2 + {\gamma_e}^2/4} s_z, \quad (7)$$

$$s^+ = \frac{(\Omega a^+ + G{d_m}^+)(2\Delta - i\gamma_e)}{\Delta^2 + {\gamma_e}^2/4} s_z. \quad (8)$$

Combining Equation (3), we can obtain the steady-state pseudospin operator s_z of QD:

$$s_z = -\frac{1}{2}\frac{1}{1 + y_m}, \quad (9)$$

where $y_m = n_t / P_{\text{ctm}}$ and $P_{\text{ctm}} = \frac{k_2(\Delta^2 + \gamma_e^2/4)}{2\Omega^2}$. Therefore, by integrating Equations (3)–(6) and using Equations (7)–(9), the input–output relation between n_{in} and n_t can be finally solved as

$$n_{in} = -\frac{n_t}{k_1 k_2}\left[O - (k + \frac{\gamma_{\text{cav}}}{2})\right]^2 + \left[(\Delta + \delta) - P + \frac{\Omega D_2}{G D_1}\right]^2. \quad (10)$$

In Equation (10), the new variables $D_1 = \Delta^2 + \gamma_e^2/4$, $D_2 = 2(\gamma_e/2 - i\Delta)G\Omega$, $O = 2D_1G^2(J^2D_1 + JD_2)s_z - D_1(D_2J + D_2^2/D_1)(\Delta + \delta)$, $P = D_1(\Delta + \delta)(J^2D_1 + JD_2) + 2D_1G^2\,(D_2J + D_2^2/D_1)s_z$ are introduced for simplicity. In the following calculation, we will use the parameters normalized by the decay rate $\gamma_e = 1$.

3. Results and Discussions

By employing optical nonlinearity in an asymmetric cavity system, optical nonreciprocity can be achieved in two reverse transmission directions [41,42,78]. Here we focus on the optical nonreciprocal transmission of few photons in the single QD-MNP-composed ring cavity system. The input–output relationship can be obtained easily via solving Equation (10) directly. We firstly consider the light transmissions along the forward direction, i.e., the direction from left to right. The cavity mirrors M_1 and M_2 are assumed to be asymmetrical by making their loss rates $k_1 \neq k_2$. Figure 2 shows dependence of n_t on n_{in} in the single QD–cavity system and the QD-MNP–cavity system, respectively. In the calculation of Figure 2, we have set the other parameters $\Delta = \delta = \gamma_{\text{cav}} = 0$, $\Omega = 25.0$ and $J = G = 2.0$. As shown in Figure 2a, for the case of $k_1 = 600$ and $k_2 = 400$, the optical bistability effect presents when the input photon number approaches $n_{in} = 0.8$ (see the red solid line). And for the case of $k_1 = 400$ and $k_2 = 600$, the optical bistability effect presents when the number of input photons approaches $n_{in} = 1.2$ (see the blue dashed line). Interchanging the numerical values of k_1 and k_2 corresponds the two cases of forward and backward light transmission, respectively. With the help of the surface plasmon effect provided by the MNP, the number of photons required to generate optical bistability can be significantly reduced because of the significantly enhanced optical nonlinearity in the system. As shown in Figure 2b, the required number of photons has been reduced to around $n_{in} \approx 0.14$ and $n_{in} \approx 0.21$, respectively, for the two same cases as in Figure 2a. Therefore, due to the different bistable curves and threshold in the two cases (two reverse directions), it is possible to achieve quantum nonreciprocity in the hybrid QD-MNP–cavity system with extremely few photons. We can obtain high transmission of the light in one direction and significantly suppress the light transmission in the opposite direction.

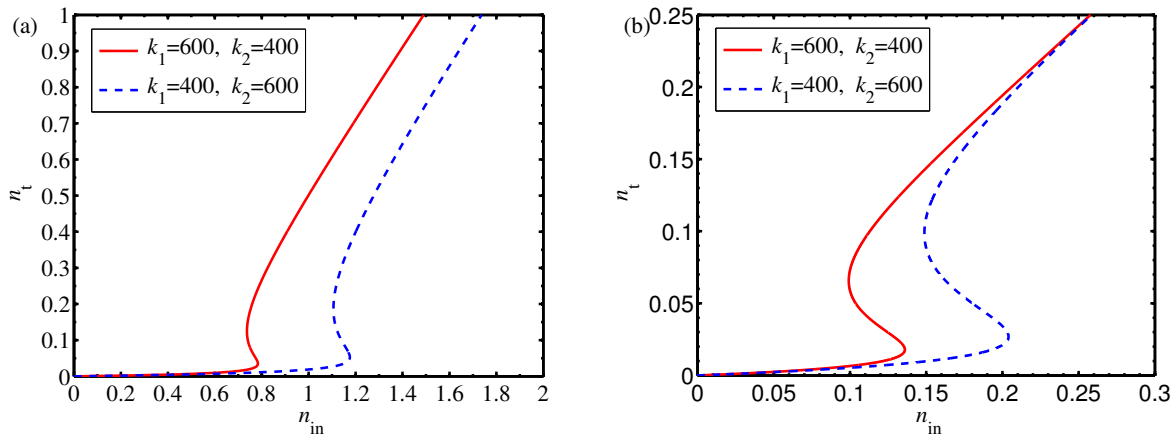


Figure 2. (Color online) variations of n_t with n_{in} in (**a**) the single QD–cavity system and (**b**) the QD-MNP–cavity system. The parameters are set as $\Delta = \delta = \gamma_{\text{cav}} = 0$, $\Omega = 25.0$, and $J = G = 2.0$. The red solid and blue dashed curves correspond to $k_1, k_2 = 600, 400$ and $400, 600$, respectively.

Transmittance is an important indicator for evaluating performance of the optical nonreciprocity. The transmittance can be determined by calculating $T_i(i = f, b) = n_t/n_{in}$, where $(i = f, b)$ stands for the forward/backward direction. From Figure 2, the forward transmittance can be estimated to be approximately $T_f \sim 50\%$ in the single QD–cavity system, while it exceeds 90% in the QD–MNP–cavity system. To further characterize the nonreciprocal behavior, the isolation is defined as $I = 10\log_{10}(T_f/T_b)$, where a larger isolation corresponds to stronger nonreciprocal performance. The maximum isolation in the single QD–cavity system is about 2.44 dB, whereas the QD–MNP–cavity system can achieve an isolation above 11.69 dB, demonstrating that the incorporation of the MNP improves the nonreciprocal performance of the system. We further calculate the transmittance T_i for the forward and backward directions in the QD-MNP–cavity system, and display it in Figure 3, where the red solid line and the blue dashed line correspond to the forward and backward transmissions, respectively. It is evident that high transmission in the forward direction and suppressed transmission in the backward direction can be simultaneously achieved within a certain range of n_{in}. From Figure 3, we can easily find a range of input photon number for quantum nonreciprocity (as denoted by the black dotted vertical lines in Figure 3), in which more than 95% forward transmission and nearly vanishing backward transmission can be attained within $n_{in} \in [0.136, 0.149]$. We also calculate the backward isolation and obtain $I \approx 11.87$ dB at $n_{in} = 0.149$, indicating good isolation effect in the backward direction. Therefore, utilizing the optical bistability enhanced by the surface plasmon effect, we can achieve nonreciprocal transmission at the few-photon level in this system, which provides the possibility of fabricating single-photon nonreciprocal devices.

The nonreciprocal property depends sensitively on the cavity loss rates k_1 and k_2. We investigate the influences of the cavity loss rate k_1 and k_2 on the nonreciprocal transmission, and show the results in Figure 4. Figure 4a displays variation of n_t with n_{in} under different cavity loss rates k_1 and k_2, and Figure 4b displays variation of $T_f(T_b)$ with n_{in} for the forward/backward directions corresponding to three different cases (case 1: $k_1 = 600$, $k_2 = 400$; case 2: $k_1 = 700$, $k_2 = 300$; case 3: $k_1 = 800$, $k_2 = 200$). Obviously, it can be seen that, with the increase of k_1 and decrease of k_2, the nonreciprocal region is significantly expanded and the threshold for generating nonreciprocity is remarkably reduced. That is because more photons enter the cavity and participate in the nonlinear processes in the forward direction. On the other hand, fewer photons enter the cavity in the opposite direction. So, the nonreciprocal region is expanded with the increase in asymmetry of the cavity loss rates, which is of course desired for the nonreciprocal transmission. But the

decrease in forward transmittance that accompanies it is not what nonreciprocal transmission expects. Therefore, there also needs to be a trade-off between high transmittance and nonreciprocal interval.

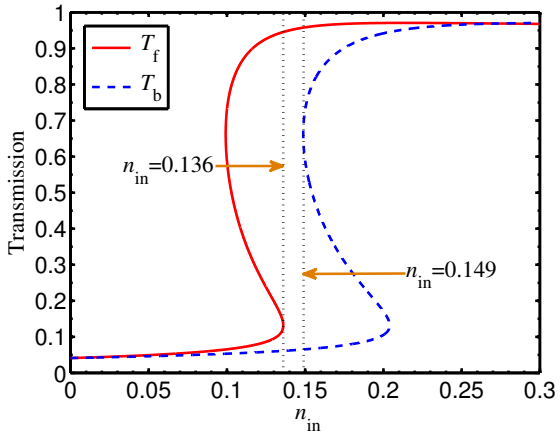


Figure 3. (Color online) variation in the transmittance T_i with n_{in} for the forward and backward directions in the QD-MNP–cavity system. The red solid and blue dashed curves represent the forward T_f and backward T_b transmissions, respectively. The black dotted lines indicate the region of quantum nonreciprocity. The other parameters are the same as in Figure 2b.

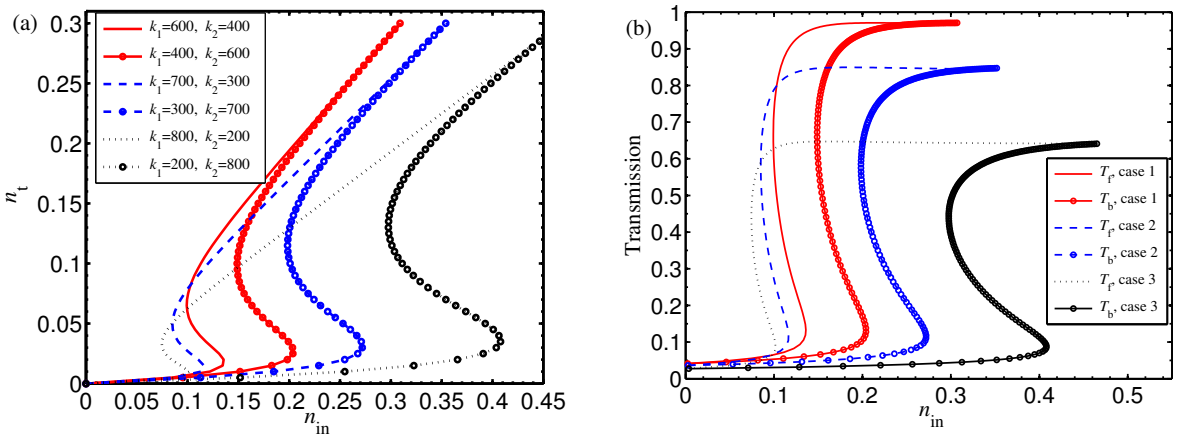


Figure 4. (Color online) variations of (**a**) n_t and (**b**) $T_f(T_b)$ with n_{in} under different asymmetric cavity loss rates in the QD-MNP–cavity system. For (**b**), case 1, case 2, and case 3 correspond to $k_1, k_2 = 600, 400$; $k_1, k_2 = 700, 300$; and $k_1, k_2 = 800, 200$, respectively. The other parameters are the same as in Figure 3.

We further investigate the effects of the laser detuning Δ and the coupling coefficients Ω, J and G on the quantum nonreciprocity, and show the results in Figure 5. As shown in Figure 5a, negative and positive laser detuning Δ play different roles in the forward and backward transmission. For $\Delta = -0.5$, the optical bistable curves exhibit a small gain within a certain range of input photon number (red solid lines). Though the asymmetric bistable curves for the forward/backward still exist, effective nonreciprocal transmission can no longer be achieved because the bistable regions of the two transmission curves overlap near $n_{in} = 0.211$, as denoted by the black dotted–dashed line. It is obvious that the effective nonreciprocal interval for $\Delta = 0.5$ (black dotted lines) is increased in comparison with that of $\Delta = 0$ (blue dashed lines). However, for the case of $\Delta = 0.5$, a decrease in the forward transmission and an increase in the backward transmission will reduce the nonreciprocal performance. At the same time, the number of photons required to generate ONR also increases. From Figure 5b, it can be seen that the magnitude of coupling coefficient Ω significantly changes the shape of the bistable curve, indicating a

strong sensitivity of the nonreciprocal response to Ω. The case $\Omega = 25.0$ corresponds to the optimal nonreciprocal performance in terms of both isolation ratio and transmission window. For comparison, when $\Omega = 20.0$, although the nonreciprocal interval can still be found, the increase in reverse transmission also reduces the performance of nonreciprocity (see the red solid lines). When $\Omega = 27.0$, the asymmetric bistable behavior is no longer sufficient to support optical nonreciprocal transmission, as indicated by the vertical dotted–dashed line at $n_{in} = 0.155$ (see the black dotted lines). As shown in Figure 5c, with increase of the coupling efficient J, the shape of the bistable curve has almost no change, which means it has little effect on the nonreciprocal interval. But it reduces the threshold for generating optical bistability (also the ONR), and increases the forward transmittance of nonreciprocal transmission. Figure 5d shows the influence of the coupling coefficient G on the forward/backward transmission. It can be seen that, for $G = 1.90$, the S-shaped curve of optical bistability becomes flat and the threshold decreases compared with that of $G = 2.00$, which also implies an increase of the nonreciprocal interval. For $G = 2.05$, although asymmetric optical bistability curves still exist, they cannot actually be used for nonreciprocal transmission due to reasons similar to those in Figure 5a (denoting by the black dotted–dashed vertical line of $n_{in} = 0.163$). As shown in Figure 5e, increase of γ_{cav} gradually suppresses the forward transmission and increases the backward transmission, leading to degradation of the nonreciprocal performance. Meanwhile, the bistable threshold is slightly shifted toward a larger input photon number. Nevertheless, the asymmetric transmission between the forward and backward directions is still observable within the considered parameter range, indicating that the nonreciprocal behavior persists under moderate cavity losses. Figure 5f shows the influence of δ on the forward/backward transmission. It can be seen that the cavity–QD detuning significantly changes the shape and position of the asymmetric bistable curves. For $\delta = -0.5$, the forward transmission is enhanced and the bistable threshold is reduced, leading to improved nonreciprocal transmission performance. In contrast, $\delta = 0.5$ suppresses the forward transmission and shifts the bistable region toward larger input photon number, which weakens the nonreciprocal behavior. These results demonstrate that the nonreciprocal response can be effectively modulated by the cavity–QD detuning.

Finally, we briefly discuss the experimental feasibility of the proposed QD–MNP–cavity system. The two-level quantum emitter can be realized by semiconductor quantum dots such as self-assembled InGaAs quantum dots [79]. Strong coupling between a single quantum dot and a photonic crystal nanocavity has been demonstrated experimentally [80]. In addition, hybrid QD–MNP structures can be fabricated using various nanofabrication and self-assembly techniques, with the QD–MNP separation controllable at the nanometer scale [81]. These studies suggest that the parameter regime considered in this work is physically plausible and may be accessible with current nanophotonic technologies.

Despite the experimental feasibility discussed above, it should be noted that the intrinsic dissipative losses of the metallic nanoparticle are not explicitly included in the present model. In realistic plasmonic systems, absorption and damping would introduce additional losses, which may reduce the transmission efficiency and modify the quantitative characteristics of optical nonreciprocity. Therefore, the transmission values reported here should be regarded as idealized estimates. A more complete treatment including plasmonic losses would be valuable for quantitatively assessing the device performance in practical implementations. Nevertheless, the present model provides useful insight into the nonlinear mechanism responsible for the observed nonreciprocal behavior.

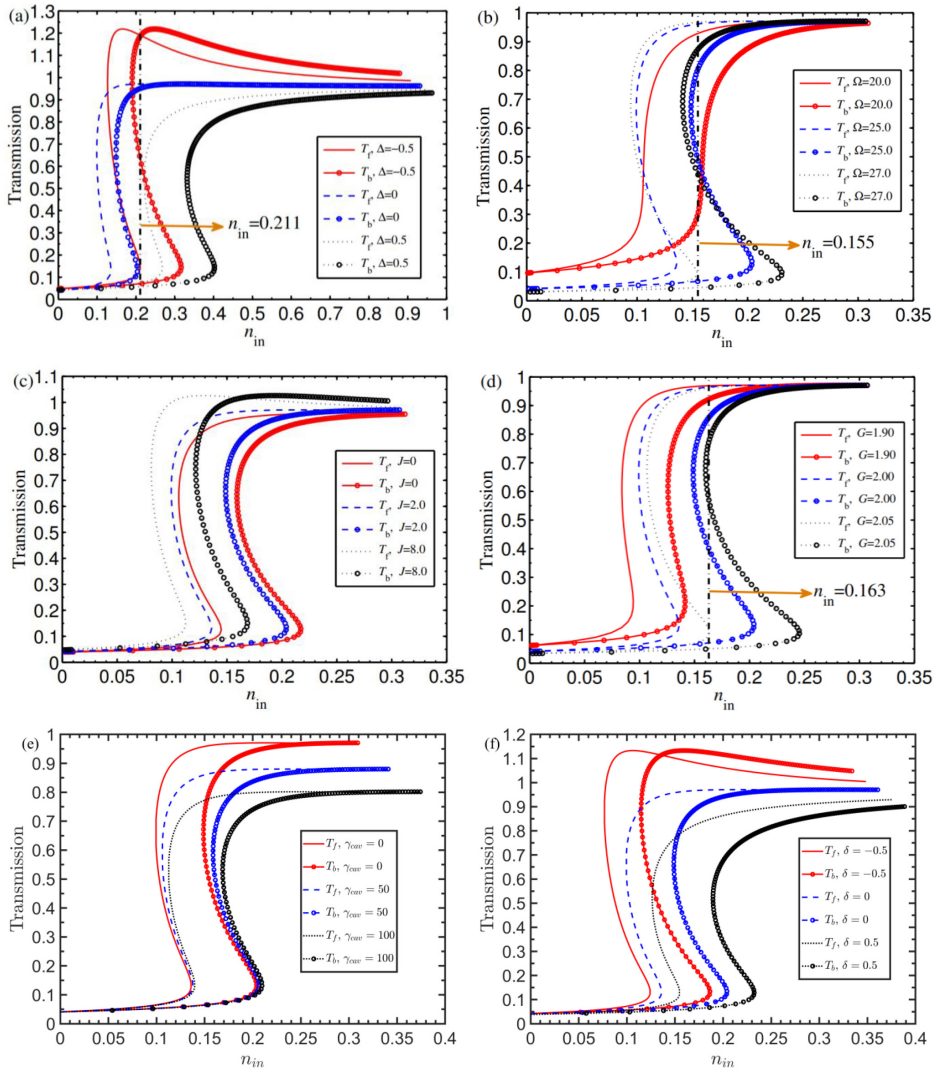


Figure 5. (Color online) influences of the laser detuning Δ, the coupling coefficients Ω, J, G, the cavity mode loss rate γ_{cav}, and the detuning δ between the cavity mode and the quantum dot transition frequency on the forward/backward nonreciprocal transmission in the QD–MNP–cavity system. Figures (**a**–**f**) correspond to the effects of Δ, Ω, J, and G, respectively. In the calculation, the parameters (**a**) $\Omega = 25.0$, $J = G = 2.0$, (**b**) $\Delta = 0$, $J = G = 2.0$, (**c**) $\Delta = 0$, $\Omega = 25.0$, $G = 2.0$, (**d**) $\Delta = 0$, $\Omega = 25.0$ and $J = 2.0$, (**e**) $\Delta = \delta = 0$, $\Omega = 25.0$, and $J = G = 2.0$, (**f**) $\Delta = 0$, $\Omega = 25.0$, $J = G = 2.0$, and $\gamma_{cav} = 0$ are selected separately, and the other parameters are the same as in Figure 3.

4. Conclusions

In conclusion, we have investigated nonlinear ONR at the few-photon level in a QD-MNP ring–cavity-coupled system. The input–output relations of the hybrid cavity quantum system are derived theoretically via solving the Heisenberg–Langevin equations. It is demonstrated that few-photon nonreciprocal transmission can be achieved via the optical bistability effect with proper parameters' range of the hybrid system. With the surface plasmon effect of the MNP, the bistable property and regime of photons producing ONR in the asymmetric ring cavity including a QD and an MNP inside can be significantly improved in comparison with the case of a single QD. By changing the loss rates of the asymmetric cavity mirrors, giant ONR can be achieved in an optimal window of numbers of input photons. We have also studied the influences of the laser detuning and the coupling coefficients Ω, J and G of the hybrid system, which demonstrates that the nonreciprocal transmission properties of few photons can be controlled and improved by adjusting

these parameters. Our work may provide references for experimental study of quantum nonreciprocity and find promising applications in quantum nonreciprocal devices and photonic quantum circuits.

Author Contributions: Conceptualization, Y.Q. and Z.L.; methodology, Z.L., Y.Q. and H.Y.; validation, Z.L., H.Y. and F.X.; investigation, Z.L.; writing—original draft preparation, Z.L. and Y.Q.; writing—review and editing, H.Y. and Y.Q.; supervision, P.W. and Y.Q.; project administration, Y.Q.; funding acquisition, Y.Q. and P.W. All authors have read and agreed to the published version of the manuscript.

Funding: This research was funded by the National Natural Sciences Foundation of China (Grant Nos. 12274123 and 11874146) and the Anhui Provincial Universities Natural Science Research Project (Grant No. KJ2019A0567).

Data Availability Statement: Data are contained within the article

Conflicts of Interest: The authors declare no conflicts of interest.

References

1. Potton, R.J. Reciprocity in optics. *Rep. Prog. Phys.* **2004**, *67*, 717–754. [CrossRef]
2. Sounas, D.L.; Alù, A. Non-reciprocal photonics based on time modulation. *Nat. Photon.* **2017**, *11*, 774–783. [CrossRef]
3. Bi, L. Materials for nonreciprocal photonics. *MRS Bull.* **2018**, *43*, 408–412. [CrossRef]
4. Yu, M.; Cheng, R.; Reimer, C.; He, L.; Luke, K.; Puma, E.; Shao, L.; Shams-Ansari, A.; Ren, X.; Grant, H.R.; et al. Integrated electro-optic isolator on thin-film lithium niobate. *Nat. Photon.* **2023**, *17*, 666–671. [CrossRef]
5. Haldane, F. D. M.; Raghu, S. Possible Realization of Directional Optical Waveguides in Photonic Crystals with Broken Time-Reversal Symmetry. *Phys. Rev. Lett.* **2008**, *100*, 013904. [CrossRef] [PubMed]
6. Wang, Z.; Chong, Y.; Joannopoulos, J.D.; Soljačić, M. Observation of unidirectional backscattering-immune topological electromagnetic states. *Nature* **2009**, *461*, 772–775. [CrossRef] [PubMed]
7. Wen, J.; Jiang, X.; Zhang, M.; Jiang, L.; Hua, S.; Wu, H.; Yang, C.; Xiao, M. Modeling of on-chip optical nonreciprocity with an active microcavity. *Photonics* **2015**, *2*, 498–508. [CrossRef]
8. Xue, M.; Tong, H.; Dong, H.; Wang, M. Saturated gain-induced non-reciprocal transmission and broadband on-chip optical isolator. *Photonics* **2024**, *11*, 261.
9. Yu, Z.; Fan, S. Complete optical isolation created by indirect interband photonic transitions. *Nat. Photon.* **2009**, *3*, 91–94. [CrossRef]
10. Tzuang, L.D.; Fang, K.; Nussenzveig, P.; Fan, S.H.; Lipson, M. Non-reciprocal phase shift induced by an effective magnetic flux for light. *Nat. Photon.* **2014**, *8*, 701–705. [CrossRef]
11. Estep, N.A.; Sounas, D.L.; Soric, J.; Alù, A. Magnetic-free non-reciprocity and isolation based on parametrically modulated coupled-resonator loops. *Nat. Phys.* **2014**, *10*, 923–927.
12. Wang, D.W.; Zhou, H.T.; Guo, M.J.; Zhang, J.X.; Evers, J.; Zhu, S.Y. Optical diode made from a moving photonic crystal. *Phys. Rev. Lett.* **2013**, *110*, 093901. [CrossRef]
13. Wu, J.H.; Artoni, M.; La Rocca, G.C. Non-Hermitian degeneracies and unidirectional reflectionless atomic lattices. *Phys. Rev. Lett.* **2014**, *113*, 123004. [CrossRef]
14. Zhang, H.L.; Zhang, H.J.; Chen, X.N.; Li, Y.B.; Xu, P.P.; Li, H.B.; Sun, H. Nonreciprocal transmission of single-photon in a spinning resonator coupled to a qubit four-port photonic system. *Opt. Laser Technol.* **2026**, *199*, 114990. [CrossRef]
15. Chang, L.; Jiang, X.; Hua, S.; Yang, C.; Wen, J.M.; Jiang, L.; Li, G.Y.; Wang, G.Z.; Xiao, M. Parity–time symmetry and variable optical isolation in active–passive-coupled microresonators. *Nat. Photon.* **2014**, *8*, 524–529. [CrossRef]
16. Peng, B.; Özdemir, S.K.; Lei, F.; Monifi, F.; Gianfreda, M.; Long, G.L.; Fan, S.H.; Nori, F.; Bender, C.M.; Yang, L. Parity–time-symmetric whispering-gallery microcavities. *Nat. Phys.* **2014**, *10*, 394–398.
17. Guo, X.; Zou, C.L.; Jung, H.; Tang, H.X. On-chip strong coupling and efficient frequency conversion between telecom and visible optical modes. *Phys. Rev. Lett.* **2016**, *117*, 123902. [CrossRef]
18. Xia, K.; Nori, F.; Xiao, M. Cavity-Free Optical Isolators and Circulators Using a Chiral Cross-Kerr Nonlinearity. *Phys. Rev. Lett.* **2018**, *121*, 203602. [CrossRef]
19. Lin, Z.L.; Yang, H.; Xu, F.; Qi, Y.H.; Niu, Y.P.; Gong, S.Q. Optical nonreciprocity based on the four-wave mixing effect in semiconductor quantum dots. *Nanomaterials* **2025**, *15*, 380. [CrossRef]
20. Shen, Z.; Zhang, Y.L.; Chen, Y.; Zou, C.L.; Xiao, Y.F.; Zou, X.B.; Sun, F.W.; Guo, G.C.; Dong, C.H. Experimental realization of optomechanically induced non-reciprocity. *Nat. Photon.* **2016**, *10*, 657–661. [CrossRef]

21. He, B.; Yang, L.; Jiang, X.; Xiao, M. Transmission nonreciprocity in a mutually coupled circulating structure. *Phys. Rev. Lett.* **2018**, *120*, 203904. [CrossRef] [PubMed]
22. Maayani, S.; Dahan, R.; Kligerman, Y.; Moses, E.; Hassan, A.U.; Jing, H.; Nori, F.; Christodoulides, D.N.; Carmon, T. Flying couplers above spinning resonators generate irreversible refraction. *Nature* **2018**, *558*, 569–574. [CrossRef]
23. Ullah, M.; Mikki, S. Optical nonreciprocity in a multimode cavity optomechanical system controlled by dynamic casimir force. *Adv. Quantum Technol.* **2024**, *7*, 2400007. [CrossRef]
24. Liu, Z.X.; Wei, D.; Sun, J.H. Nonreciprocal microcombs via spinning optomechanics. *New J. Phys.* **2026**, *28*, 014516. [CrossRef]
25. Kongkui Berinyuy, E.; Peng, J.X.; Djorwé, P.; Abdourahimi; Abdel-Aty, A.H.; Nisar, K.S.; Nana Engo, S.G. Nonreciprocal transmission in hybrid atomic ensemble-optomechanical systems. *Quantum Inf. Process.* **2025**, *24*, 160. [CrossRef]
26. Xia, K.; Lv, G.; Lin, G.; Cheng, Y.; Niu, Y.; Gong, S.; Twamley, J. Reversible nonmagnetic single-photon isolation using unbalanced quantum coupling. *Phys. Rev. A* **2014**, *90*, 043802. [CrossRef]
27. Lodahl, P.; Mahmoodian, S.; Stobbe, S.; Rauschenbeutel, A.; Schneeweiss, P.; Volz, J.; Pichler, H.; Zoller, P. Chiral quantum optics. *Nature* **2017**, *541*, 473–480. [CrossRef]
28. You, Y.; Hu, Y.; Lin, G.; Qi, Y.; Niu, Y.; Gong, S. Quantum nonreciprocity based on electromagnetically induced transparency in chiral quantum-optical systems. *Phys. Rev. A.* **2021**, *103*, 063706.
29. Zhang, S.; Hu, Y.; Lin, G.; Niu, Y.; Xia, K.; Gong, J.; Gong, S. Thermal-motion-induced non-reciprocal quantum optical system. *Nat. Photon.* **2018**, *12*, 744–748.
30. Lin, G.; Zhang, S.; Hu, Y.; Niu, Y.; Gong, J.; Gong, S. Nonreciprocal amplification with four-level hot atoms. *Phys. Rev. Lett.* **2019**, *123*, 033902. [CrossRef]
31. Fan, S.; Qi, Y.; Lin, G.; Niu, Y.; Gong, S. Broadband optical nonreciprocity in an N-type thermal atomic system. *Opt. Commun.* **2020**, *462*, 125343. [CrossRef]
32. Liang, C.; Liu, B.; Xu, A.N.; Wen, X.; Lu, C.C.; Xia, K.Y.; Tey, M.K.; Liu, Y.C.; You, L. Collision-induced broadband optical nonreciprocity. *Phys. Rev. Lett.* **2020**, *125*, 123901. [CrossRef]
33. Zhang, S.; Lin, G.; Hu, Y.; Qi, Y.; Niu, Y.; Gong, S. Cavity-free circulator with low iInsertion loss using hot atoms. *Phys. Rev. Appl.* **2021**, *14*, 024032.
34. Hu, Y.; Zhang, S.; Kuang, X.; Qi, Y.; Lin, G.; Gong, S.; Niu, Y. Reconfigurable nonreciprocity with low insertion loss using a simple two-level system. *Opt. Express* **2020**, *28*, 409850. [CrossRef]
35. Dong, M.X.; Xia, K.Y.; Zhang, W.H.; Yu, Y.C.; Ye, Y.H.; Li, E.Z.; Zeng, L.; Ding, D.S.; Shi, B.S.; Guo, G.C.; et al. All-optical reversible single-photon isolation at room temperature. *Sci. Adv.* **2021**, *7*, eabe8924. [CrossRef]
36. Lin, K.S.; Gao, G.F.; Gao, Y.; Li, Z.L.; Jiang, X.F. Passive all-optical isolator based on spatial self-phase modulation. *Opt. Lett.* **2025**, *50*, 2727–2730. [CrossRef]
37. Wang, Z.B.; Zhang, Y.L.; Hu, X.X.; Chen, G.J.; Li, M.; Yang, P.F.; Zou, X.B.; Zhang, P.F.; Dong, C.H.; Li, G.; et al. Self-induced optical non-reciprocity. *Light Sci. Appl.* **2025**, *14*, 23.
38. Fan, L.; Wang, J.; Varghese, L.T.; Shen, H.; Niu, B.; Xuan, Y.; Weiner, A.M.; Qi, M.H. An all-silicon passive optical diode. *Science* **2012**, *335*, 447. [CrossRef]
39. Hu, X.; Xin, C.; Li, Z.; Gong, Q. Ultrahigh-contrast all-optical diodes based on tunable surface plasmon polaritons. *New J. Phys.* **2010**, *12*, 023029.
40. Zhou, X.; Wang, Y.; Leykam, D.; Chong, Y.D. Optical isolation with nonlinear topological photonics. *New J. Phys.* **2017**, *19*, 095002. [CrossRef]
41. Yang, P.; Xia, X.; He, H.; Li, S.K.; Han, X.; Zhang, P.; Li, G.; Zhang, P.F.; Xu, J.P.; Yang, Y.P.; et al. Realization of nonlinear optical nonreciprocity on a few-photon level based on atoms strongly coupled to an asymmetric cavity. *Phys. Rev. Lett.* **2019**, *123*, 233604. [CrossRef]
42. Hu, Y.; Qi, Y.; You, Y.; Zhang, S.; Lin, G.; Li, X.; Gong, J.; Gong, S.; Niu, Y. Passive nonlinear optical isolators bypassing dynamic reciprocity. *Phys. Rev. Appl.* **2021**, *16*, 014046. [CrossRef]
43. Sounas, D.L.; Soric, J.; Alù, A. Broadband passive isolators based on coupled nonlinear resonances. *Nat. Electron.* **2018**, *1*, 113–119. [CrossRef]
44. Yang, K.Y.; Skarda, J.; Cotrufo, M.; Dutt, A.; Ahn, G.H.; Sawaby, M.; Vercruysse, D.; Arbabian, A.; Fan, S.H.; Alù, A.; et al. Inverse-designed non-reciprocal pulse router for chip-based LiDAR. *Nat. Photon.* **2020**, *14*, 369–374. [CrossRef]
45. Liu, Y.L.; Zhang, K.K.; Zhao, R.S.; Fei, X.L.; Liu, X.C.; Jia, Z.Y.; Liu, X.Y.; Xie, X.T. Nonreciprocal frequency combs by two-photon driving in cavity magnonics. *Opt. Lett.* **2025**, *50*, 4234–4237. [CrossRef]
46. Benson, O. Assembly of hybrid photonic architectures from nanophotonic constituents. *Nature* **2011**, *480*, 193–199. [CrossRef]
47. Chang, D.E.; Sørensen, A.S.; Demler, E.A.; Lukin, M.D. A single-photon transistor using nanoscale surface plasmons. *Nat. Phys.* **2007**, *3*, 807–812. [CrossRef]
48. Liu, R.; Zhou, Z.K.; Yu, Y.C.; Zhang, T.W.; Wang, H.; Liu, G.H.; Wei, Y.M.; Chen, H.J.; Wang, X.H. Strong light-matter interactions in single open plasmonic nanocavities at the quantum optics limit. *Phys. Rev. Lett.* **2017**, *118*, 237401. [CrossRef]

49. Artuso, R.D.; Bryant, G.W. Optical response of strongly coupled quantum dot-metal nanoparticle systems: Double peaked fano structure and bistability. *Nano Lett.* **2008**, *8*, 2106–2111.
50. Ridolfo, A.; Di Stefano, O.; Fina, N.; Saija, R.; Savasta, S. Quantum plasmonics with quantum dot-metal nanoparticle molecules: Influence of the Fano effect on photon statistics. *Phys. Rev. Lett.* **2010**, *105*, 263601. [CrossRef]
51. Akimov, A.V.; Mukherjee, A.; Yu, C.L.; Chang, D.E.; Zibrov, A.S.; Hemmer, P.R.; Park, H.; Lukin, M.D. Generation of single optical plasmons in metallic nanowires coupled to quantum dots. *Nature* **2007**, *450*, 402. [CrossRef]
52. Paspalakis, E.; Evangelou, S.; Yannopapas, V.; Terzis, A.F. Phase-dependent optical effects in a four-level quantum system near a plasmonic nanostructure. *Phys. Rev. A* **2013**, *88*, 053832. [CrossRef]
53. Carreño, F.; Antón, M.A.; Yannopapas, V.; Paspalakis, E. Resonance fluorescence spectrum of a Λ-type quantum emitter close to a metallic nanoparticle. *Phys. Rev. A* **2016**, *94*, 013834. [CrossRef]
54. Hatef, A.; Sadeghi, S.M.; Singh, M.R. Plasmonic electromagnetically induced transparency in metallic nanoparticle–quantum dot hybrid systems. *Nanotechnology* **2012**, *23*, 065701. [CrossRef]
55. Li, J.; Shen, S.; Ding, C.; Wu, Y. Magnetically induced optical transparency in a plasmon-exciton system. *Phys. Rev. A* **2021**, *103*, 053706. [CrossRef]
56. Savasta, S.; Saija, R.; Ridolfo, A.; Di Stefano, O.; Denti, P.; Borghese, F. Nanopolaritons: Vacuum Rabi splitting with a single quantum dot in the center of a dimer nanoantenna. *ACS Nano* **2010**, *4*, 6369–6376. [CrossRef]
57. Santhosh, K.; Bitton, O.; Chuntonov, L.; Haran, G. Vacuum Rabi splitting in a plasmonic cavity at the single quantum emitter limit. *Nat. Commun.* **2016**, *7*, 11823. [CrossRef]
58. Artuso, R.D.; Bryant, G.W. Strongly coupled quantum dot-metal nanoparticle systems: Exciton-induced transparency, discontinuous response, and suppression as driven quantum oscillator effects. *Phys. Rev. B* **2010**, *82*, 195419. [CrossRef]
59. Zhao, D.; Wu, J.; Gu, Y.; Gong, Q. Tailoring double Fano profiles with plasmon-assisted quantum interference in hybrid exciton-plasmon system. *Appl. Phys. Lett.* **2014**, *105*, 111112. [CrossRef]
60. Paspalakis, E.; Evangelou, S.; Terzis, A.F. Control of excitonic population inversion in a coupled semiconductor quantum dot–metal nanoparticle system. *Phys. Rev. B* **2013**, *87*, 235302. [CrossRef]
61. Qi, Y.; Shu, C.; Dong, D.; Petersen, I.R.; Jacobs, K.; Gong, S. Fast quantum state transfer in hybrid quantum dot-metal nanoparticle systems by shaping ultrafast laser pulses. *J. Phys. D Appl. Phys.* **2019**, *52*, 425101.
62. Paspalakis, E.; Smponias, A.; Stefanatos, D. Coherent preparation of the biexciton state in a semiconductor quantum dot coupled to a metallic nanoparticle. *J. Appl. Phys.* **2021**, *129*, 223104. [CrossRef]
63. You, Y.; Qi, Y.; Niu, Y.; Gong, S. Control of electromagnetically induced grating by surface plasmon and tunneling in a hybrid quantum dot–metal nanoparticle system. *J. Phys. Condens. Mat.* **2019**, *31*, 105801. [CrossRef]
64. Fu, M.; Wang, K.; Long, H.; Yang, G.; Lu, P.X.; Hetsch, F.; Susha, A.S.; Rogach, A.L. Resonantly enhanced optical nonlinearity in hybrid semiconductor quantum dot–metal nanoparticle structures. *Appl. Phys. Lett.* **2012**, *100*, 063117. [CrossRef]
65. Chen, H.; Ren, J.; Gu, Y.; Zhao, D.; Zhang, J.; Gong, Q. Nanoscale Kerr nonlinearity enhancement using spontaneously generated coherence in plasmonic nanocavity. *Sci. Rep.* **2015**, *5*, 18315. [CrossRef]
66. Tiarks, D.; Baur, S.; Schneider, K.; Dürr, S.; Rempe, G. Single-photon transistor using a Förster resonance. *Phys. Rev. Lett.* **2014**, *113*, 053602. [CrossRef]
67. Kyriienko, O.; Sørensen, A.S. Continuous-wave single-photon transistor based on a superconducting circuit. *Phys. Rev. Lett.* **2016**, *117*, 140503.
68. Tang, J.S.; Nie, W.; Tang, L.; Chen, M.Y.; Su, X.; Lu, Y.Q.; Nori, F.; Xia, K.Y. Nonreciprocal single-photon band structure. *Phys. Rev. Lett.* **2022**, *128*, 203602. [CrossRef]
69. Zhang, S.; Zhan, Y.; Gong, S.; Niu, Y. Noiseless single-photon isolator at room temperature. *Commun. Phys.* **2023**, *6*, 33. [CrossRef]
70. Yang, P.; Li, M.; Han, X.; He, H.; Li, G.; Zou, C.L.; Qian, Y.H.; Zhang, T.C. Non-Reciprocal Cavity Polariton with Atoms Strongly Coupled to Optical Cavity. *Laser Photonics Rev.* **2023**, *17*, 2200574. [CrossRef]
71. Li, B.J.; Zuo, Y.L.; Kuang, L.M.; Jing, H.; Lee, C.H. Loss-induced quantum nonreciprocity. *npj Quantum Inf.* **2024**, *10*, 75. [CrossRef]
72. Zheng, J.C.; Zheng, X.W.; Hei, X.L.; Qiao, Y.F.; Yao, X.Y.; Pan, X.F.; Ren, Y.M.; Huo, X.W.; Li, P.B. Single photon isolation and nonreciprocal frequency conversion in atom-waveguide systems. *Phys. Rev. A* **2025**, *111*, 043717. [CrossRef]
73. Liu, L.F.; Zhan, Y.F.; Zhang, S.C.; Gong, S.Q.; Niu, Y.P. Lossless nonreciprocity using dual-Raman interference. *Opt. Express* **2025**, *33*, 46564–46571. [CrossRef]
74. Duan, L.M.; Kimble, H.J. Scalable photonic quantum computation through cavity-assisted interactions. *Phys. Rev. Lett.* **2004**, *92*, 127902. [CrossRef]
75. Auffèves-Garnier, A.; Simon, C.; Gérard, J.M.; Poizat, J.P. Giant Optical Non-linearity induced by a Single Two-Level System interacting with a Cavity in the Purcell Regime. *Phys. Rev. A* **2007**, *75*, 053823. [CrossRef]
76. Walls, D.F.; Milburn, G.J. *Quantum Optics*; Springer: Berlin/Heidelberg, Germany, 2007.
77. Peng, P.; Liu, Y.C.; Xu, D.; Cao, Q.T.; Lu, G.; Gong, Q.; Xiao, Y.F. Enhancing coherent light-matter interactions through microcavity-engineered plasmonic resonances. *Phys. Rev. Lett.* **2017**, *119*, 233901. [CrossRef] [PubMed]

78. Fan, S.; Zhou, F.; Xu, F.; Qi, Y.; Niu, Y.; Gong, S. Nonlinear optical nonreciprocity in a surface plasmon–exciton coupled asymmetric cavity system. *Eur. Phys. J. D* **2022**, *76*, 212.
79. Xu, X.; Wu, Y.; Sun, B.; Huang, Q.; Cheng, J.; Steel, D.G.; Bracker, A.S.; Gammon, D.; Emary, C.; Sham, L.J. Fast spin state initialization in a singly charged InAs-GaAs quantum dot by optical cooling. *Phys. Rev. Lett.* **2007**, *99*, 097401. [CrossRef]
80. Ohta, R.; Ota, Y.; Nomura, M.; Kumagai, N.; Ishida, S.; Iwamoto, S.; Arakawa, Y. Strong coupling between a photonic crystal nanobeam cavity and a single quantum dot. *Appl. Phys. Lett.* **2011**, *98*, 17. [CrossRef]
81. Kuzyk, A.; Robert, S.; Fan, Z.; Pardatscher, G.; Roller, E.; Alexander Högele, A.; Simmel, F.C.; Govorov, A.O.; Liedl, T. DNA-based self-assembly of chiral plasmonic nanostructures with tailored optical response. *Nature* **2012**, *483*, 311–314. [CrossRef]

Disclaimer/Publisher's Note: The statements, opinions and data contained in all publications are solely those of the individual author(s) and contributor(s) and not of MDPI and/or the editor(s). MDPI and/or the editor(s) disclaim responsibility for any injury to people or property resulting from any ideas, methods, instructions or products referred to in the content.